Journal Pre-proof

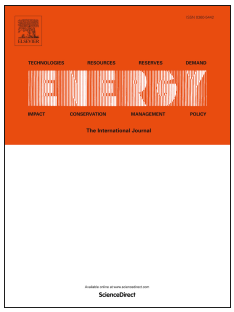

Building a net-zero power system under future climate conditions with data-driven forecasting and adequacy assessment

Jinning Lyu, Jinhui Ren, Shu Zhang, Wenying Chen

PII: S0360-5442(26)01224-7

DOI: https://doi.org/10.1016/j.energy.2026.141119

Reference: EGY 141119

To appear in: *Energy*

Received Date: 10 November 2025

Revised Date: 3 March 2026

Accepted Date: 20 April 2026

Please cite this article as: Lyu J, Ren J, Zhang S, Chen W, Building a net-zero power system under future climate conditions with data-driven forecasting and adequacy assessment, *Energy*, https://doi.org/10.1016/j.energy.2026.141119.

Building a net-zero power system under future climate conditions with data-driven forecasting and adequacy assessment

Jinning Lyu[1,2], Jinhui Ren[1,2], Shu Zhang[1,2], Wenying Chen[1,2*]
1 Institute of Energy, Environment and Economy, Tsinghua University, Beijing, 100084, China
2 Research Center for Contemporary Management, Tsinghua University, Beijing 100084, China
E-mail address: chenwy@tsinghua.edu.cn (Wenying Chen)
Address: Tsinghua University, Beijing, 100084, China

Abstract

As global energy systems transition toward carbon neutrality, the increasing variability of renewable generation and climate-sensitive load poses significant challenges to net-zero power system adequacy. However, current assessments often lack a framework that captures high-resolution, long-term load dynamics alongside transmission and storage constraints under future climate conditions. This study constructs an integrated assessment framework to evaluate the adequacy of a net-zero power system by coupling high-resolution load forecasting with power system simulations. We first developed a neural network-based Hourly Electricity Load Model (HELM) for China to forecast provincial load under diverse socioeconomic and climate scenarios. These forecasts were then integrated into an 8760-hour simulation model encompassing 30 provinces to assess system performance under more than 300 configurations of interprovincial transmission and energy storage for each carbon-neutral transition scenario. Results show that national electricity demand will reach 23262.59 TWh in 2060, with a summer peak of 3234 GW, revealing the challenges ahead in demand volatility and rising peak loads. In a power system dominated by wind and solar power, substantial spatiotemporal mismatches lead to potential electricity deficits of up to 59.54%. Targeted expansion of transmission and storage can mitigate these gaps, enhancing national system adequacy by 16.25% and exceeding 50% in power-importing provinces such as Zhejiang. These findings provide a strategic roadmap for China's energy transition by emphasizing the coordinated development of interprovincial infrastructure, flexible resources, and market-based support mechanisms.

Keywords

Net-zero power system, Electricity load forecasting, Machine learning, System adequacy, Interprovincial transmission, Energy storage

1. Introduction

To address climate change, the global energy system is undergoing a profound transformation centered on deep decarbonization [1]. On the demand side, as electrification levels steadily increase, electricity demand has grown significantly. Due to the concentrated energy consumption patterns of heating and cooling loads, peak loads have grown faster than total loads in recent years. In 2024,

China's annual electricity demand reached 9852.10 TWh [2]. On the supply side, renewable energy is widely regarded as the primary power source of future net-zero power systems, particularly wind and solar generation [3]. However, their output exhibits inherent intermittency and variability, which remain critical issues [4]. Climate change further exacerbates the spatial mismatch between resources and demand by affecting climate-sensitive cooling and heating demands [5] and intensifying variability in renewable output [6]. Future power systems will face compound risks from hard-to-predict load [7], hard-to-dispatch power plants [8], and climate-driven variability [9], all of which may further exacerbate hourly power supply-demand mismatches. Therefore, it is essential to assess provincial supply-demand matching (i.e., system adequacy) based on climate-sensitive load and renewables-dominated generation forecasting, while taking transmission and storage into account, to support the establishment of an adequate net-zero power system.

Accurate electricity load forecasting is essential for power system planning and operation. In China's evolving economy, predicting electricity load at high spatiotemporal resolution and over long-term horizons is challenging [10]. Electricity load is shaped by various factors, including economic development, regional location, climate conditions, and industrial layout [11]. Daily and especially hourly fluctuations in electricity load are primarily driven by climate-driven heating and cooling demands [12]. Traditional long-term electricity load forecasting mainly relies on statistical methods or time series analysis [13], which are limited in capturing the nonlinear and volatile nature of actual load variations [14]. Intelligent approaches leverage data-driven techniques to construct more comprehensive forecasting models. Machine learning models have been used to predict hourly or daily electricity loads [15], to assess the impacts of extreme weather in the western United States [16], or to analyze market responses in Britain [17], or to estimate daily energy demand across Australian states [18]. These studies overlooked socioeconomic dynamics, which can cause considerable inaccuracies in long-term forecasts. We bridge this gap by adapting short-term methods to produce long-term forecasts at an hourly resolution. Bloomfield, H. C. et al developed a two-stage model integrating socioeconomic trends and climate-driven fluctuations to produce national-scale demand forecasts in Europe [19]. Tang, B. et al used integrated assessment models to estimate long-term demand and quantify climate impacts using a temperature-response function [20], but only quantified the impact of extreme temperatures on building cooling and heating demand, without incorporating other meteorological factors or sectoral impacts. Overall, there is still a lack of methods capable of providing long-term provincial-level hourly electricity load forecasts in China that simultaneously account for socioeconomic trends and meteorological conditions.

As climate change increasingly affects both electricity demand [21] and renewable generation [22], integrated analyses of supply-demand matching and dispatch under climate change have become a research focus. Some studies have focused on the supply side, quantifying how wind and solar variability may lead to extreme power shortage events globally [23] or examining the fundamental temporal and spatial mismatches between renewable generation and load across 42 major countries [24]. These studies provide important groundwork for understanding the renewable-dominated power systems under climate change, yet neglect climate-sensitive demand and offer

mainly retrospective assessments. More recent analyses have taken into account both supply and demand sides for future assessment. Zhao, Z. J. et al assessed risks of supply-demand imbalance during future peak periods by quantifying unmet load from variable renewable generation, typically considering transmission but neglecting energy storage [25]. Zheng, D. et al. integrated temperature-sensitive loads with strategies such as energy storage to evaluate impacts on operational costs globally [26]. Importantly, transmission and energy storage can reduce the risk of unmet load and alleviate spatial and temporal mismatches. Existing studies rarely establish a unified modeling framework that integrates climate-sensitive load forecasting, renewable generation, transmission, and storage under future climate conditions at high spatiotemporal resolution in China.

To address these research gaps, this study established a framework to assess how an adequate net-zero power system can be achieved. We develop a provincial neural network-based Hourly Electricity Load Model (HELM) for long-term load forecasts. By capturing both climate-driven variability and heterogeneous regional development pathways, the model provides high-resolution load trajectories that better support long-term energy transition planning. We then built a simulation model to assess hourly power system supply-demand matching at the provincial level. Furthermore, rather than examining transmission expansion or energy storage in isolation, this study systematically quantifies their combined and separate roles through more than 300 configurations for each carbon-neutral transition scenario. Our focus on a wind-solar-storage configuration serves as a stress test to isolate the system-level adequacy challenges under climate change. By considering hourly climate-sensitive loads, variable renewable generation, interprovincial transmission, and energy storage at high spatiotemporal resolution, this work provides a basis for energy transition challenges in China's future net-zero power system. Section 2 provides an overview of the methodology. Section 3 provides scenario setting. Section 4 details the results. Section 5 concludes the paper, incorporating relevant discussions and policy implications.

2. Methodology

We developed an integrated framework, as illustrated in Fig. 1, comprising socioeconomic and meteorological data pre-processing modules, the Hourly Electricity Load Model (HELM), a renewable power supply module, and a net-zero power system simulation and metric evaluation module. The following subsections detail each component of this framework. The key input data and assumptions are summarized in Table 1.

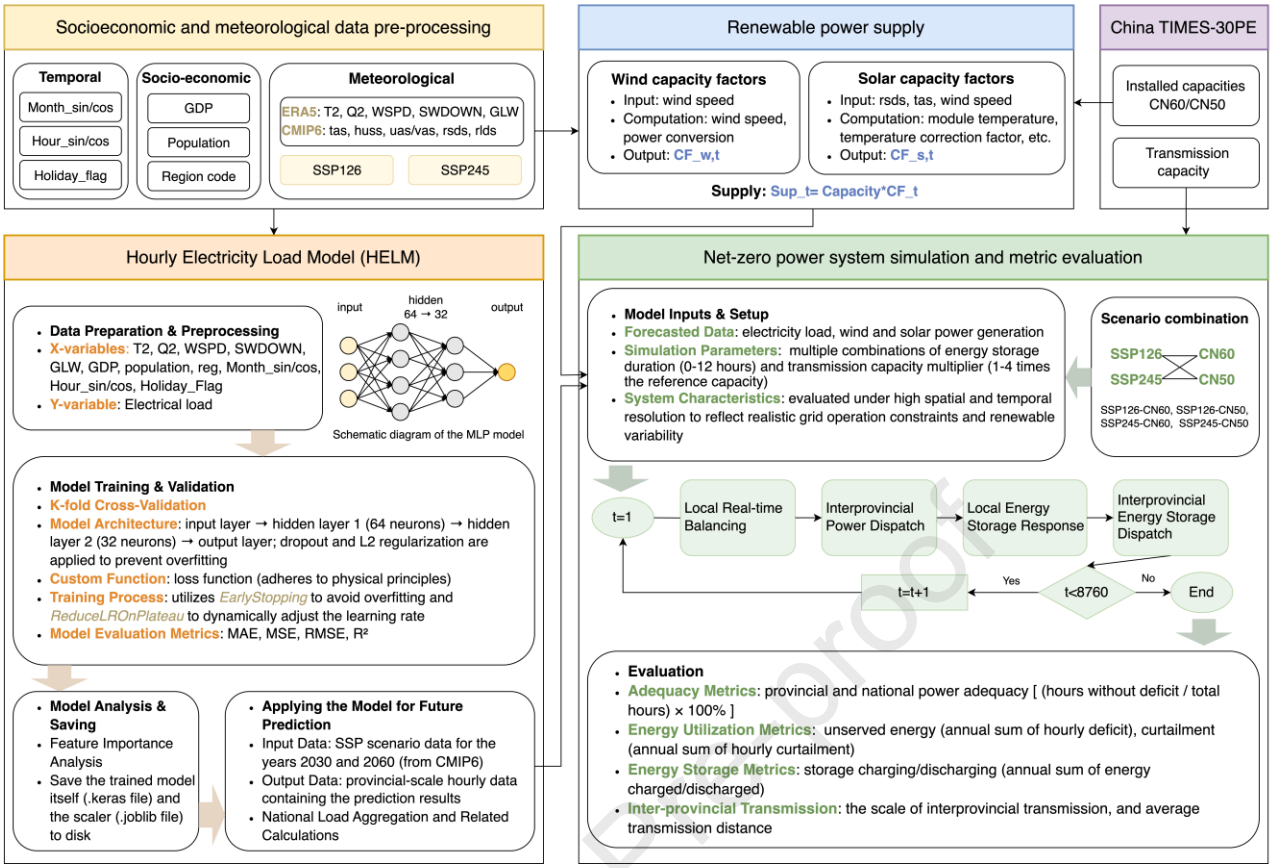

Fig. 1 | Research framework

2.1 Hourly Electricity Load Model (HELM)

We developed HELM based on a neural network implemented in TensorFlow. The original electricity load data were provincial-scale time series with 1-hour resolution for the periods 2017-2018 and 2023-2024. These data served as inputs for model training and validation. The model employs a Multi-Layer Perceptron (MLP) architecture that incorporates region code, socioeconomic variables, meteorological variables, temporal features, and holiday flags. HELM comprises two hidden layers, each with 64 and 32 neurons, respectively, using ReLU activation functions to facilitate nonlinear feature learning. A customized loss function was designed to ensure that model forecasts respect physical constraints. Overfitting was mitigated through regularization strategies: L2 regularization ($\alpha = 0.005$) and Dropout layers (rate = 0.2). Model robustness was enhanced via five-fold cross-validation, dynamic learning rate adjustment, and early stopping mechanisms. The algorithm implementation details are provided in the Supplementary Information.

Machine learning captures historical load patterns, enabling reliable long-term load forecasting under future scenarios. Model performance was evaluated using standard regression metrics, including mean absolute error (MAE), mean squared error (MSE), root mean squared error (RMSE), and the coefficient of determination (R^2). Quality control procedures included negative value filtering, minimum prediction thresholding, and diagnostics of prediction bias, including underestimation and overestimation. Permutation importance analysis was used to quantify feature

contributions, supplemented by multi-dimensional visualizations. SHAP (SHapley Additive exPlanations) was used to interpret the contribution of each input variable to the model outputs.

2.2 Simulation model for net-zero power system

We developed a 8760-hour power system simulation model for building an adequate net-zero power system, integrating climate-sensitive load and renewable generation, interprovincial transmission constraints, and energy storage deployment strategies [27] under multiple carbon-neutral transition scenarios with multi-metric performance evaluation.

The installed capacities of wind and PV are obtained from carbon-neutral transition scenarios produced by China TIMES-30PE, a provincial multi-sector energy-environment-economy model covering 2020-2060 in five-year steps [28][29]. In this study, these capacities are adjusted based on the electricity demand forecasted by HELM for the target year to align capacity levels with the load conditions. Based on the results of China TIMES-30PE, we established the reference power transmission capacity under the carbon neutrality transition scenario [28]. When storage is included, we assume that the initial and final states of charge are equal each year, thereby ensuring an energy balance between charging and discharging. Round-trip efficiency and self-discharge rate are detailed in Table 1 [30]. The maximum charging power is limited by the storage power rating, defined as the storage capacity divided by the charging duration.

The dispatch framework comprises five key components, as illustrated in a simplified workflow in Fig. S1: (i) local real-time power balancing, (ii) real-time interprovincial power dispatch, (iii) local energy storage response, (iv) interprovincial energy storage dispatch, and (v) final energy storage charging and curtailment handling. Dispatch decisions follow a gap-priority scheduling strategy and a geographic proximity-based transmission selection mechanism. The model explicitly accounts for key operational constraints of energy storage systems, including power limits, state-of-charge (SOC) dynamics, round-trip efficiency losses, and hourly degradation.

To evaluate the adequacy of the power system, we defined a set of performance metrics, including: power system adequacy (hours without deficit / total hours) × 100%), unserved energy (annual sum of hourly deficit), curtailment (annual sum of hourly curtailment), storage charging/discharging (annual sum of energy charged/discharged), the scale of interprovincial transmission, and average transmission distance.

2.3 Data collection and preprocessing

To construct inputs for the electricity load forecasting model, we utilized hourly meteorological data from the ERA5 reanalysis dataset [31] (Table 1). These variables, including temperature, humidity, wind speed, and solar radiation, were processed and converted to standard units.

For future forecasts, meteorological data were sourced from CMIP6 (BCC-CSM2-MR, r1i1p1f1) [32] (Table 1). The 3-hourly data were downscaled to an hourly resolution: rsds was interpolated using solar zenith angle-based methods with energy conservation constraints as Eqs. (1)-(3), while other variables were linearly interpolated due to their smoother temporal profiles [33]:

$$\cos(Z^t) = \sin(\delta) \cdot \sin(\phi) + cos(\delta) \cdot \cos(\phi) \cdot \cos(H^t) \quad (1)$$

$$SW_{\text{raw},t}^{1h} = SW^{3h} \cdot \frac{\cos(Z^t)}{\frac{1}{3}\sum_{t=1}^{3} \cos(Z^t)} \quad (2)$$

$$SW_t^{1h} = SW_{\text{raw}}^{1h} \cdot \frac{SW^{3h}}{\frac{1}{3}\sum_{t=1}^{3} SW_{\text{raw}}^{1h}} \quad (3)$$

Eq. (1) computes the cosine of the solar zenith angle (Z^t) for each hour using solar declination (δ), latitude (ϕ), and hour angle (H^t), thereby capturing the position of the sun relative to each grid point. Eq. (2) generates a preliminary hourly radiation distribution within each 3-hour window by proportionally allocating the total 3-hour radiation (SW^{3h}) based on solar geometry. Eq. (3) scales the raw hourly values, ensuring that the average of the disaggregated hourly values equals the original input. Meteorological variables were aggregated to the provincial level using area-weighted averaging across all grid cells within each administrative boundary.

Socioeconomic data consisted of historical provincial GDP and population data from the China Statistical Yearbook [34][35]. Future socioeconomic data were projected based on historical data and trends up to 2024, with growth rates set according to existing models and literature [28][36][37].

The capacity factors for wind and solar power represent the ratio of actual power output to the rated nameplate capacity, reflecting the resource potential of wind and solar power at a specific location. For wind capacity factors, wind speed at hub height was estimated by extrapolating from near-surface wind data as Eq. (4):

$$V_H = V_h \times (H/h)^{\alpha} \quad (4)$$

with α as the empirically validated wind shear exponent, which characterizes the variation of wind speed with height and is influenced by factors such as surface roughness. Wind speed is adjusted using dry and moist air density, specific humidity, and the reference air density corresponding to the wind turbine power curve. The wind capacity factor was then computed using a piecewise function comprising five operational regimes: (i) cut-in phase (<3 m s^{-1}): output is zero, (ii) ramp-up phase (3-5 m s^{-1}): output increases linearly from 0% to 10% of rated capacity, (iii) power growth phase (5-12 m s^{-1}): output follows a quadratic increase curve, (iv) rated operation phase (12-25 m s^{-1}): turbines operate at full capacity, (v) cut-out phase (>25 m s^{-1}): turbines shut down to avoid mechanical stress [38].

For solar capacity factors, we primarily consider utility-scale photovoltaic systems. Solar capacity factor depends largely on in-panel irradiance and operational temperature [39] as Eq. (5):

$$CF_s = (S_{avg}/1000) * TEM_{coef} * 0.85 \quad (5)$$

where CF_s denotes solar capacity factor; $S_{avg}/1000$ refers to standardized solar radiation; η_{sys}=0.85 accounts for inverter losses and other system inefficiencies; TEM_{coef} is a function of actual photovoltaic cell temperature (T_{cell}) that relies mainly on irradiation, ambient temperature, as well as surface wind speed [40] as Eqs. (6) and (7):

$$TEM_{coef} = 1 + \lambda \times (T_{cell} - T_{STC}) \quad (6)$$

$$T_{cell} = c_1 + c_2 \times T_2 + c_3 \times S_{avg} + c_4 \times V_2 \quad (7)$$

where λ denotes the typical temperature response efficiency for monocrystalline silicon modules ($-0.005\ °C^{-1}$); T_{STC} is photovoltaic cell temperature under standard test condition (25 °C), and T_{cell} represents the actual photovoltaic cell temperature (°C); c_1 is a constant (4.3 °C); c_2, c_3, and c_4 refer to temperature coefficient (0.943), irradiation coefficient (0.028 °C m^{-2} W^{-1}), and wind speed coefficient (-1.528 °C m^{-1}), respectively; T_2 and V_2 indicate ambient temperature at 2-meter height and wind speed at 2 m above ground level, respectively.

Both wind and solar capacity factors were computed at the native grid resolution before being aggregated at the provincial scale. The spatial integration employs area-weighted averaging across all grid cells within administrative boundaries [41], preserving localized meteorological heterogeneity while enabling the assessment of regional energy potential.

Installed wind and solar capacities are used to calculate hourly wind and solar supply by multiplying the hourly wind and solar capacity factors, as shown in Eqs. (8) and (9):

$$Sup_{w,t} = Capacity_w \times CF_{w,t} \quad (8)$$

$$Sup_{s,t} = Capacity_s \times CF_{s,t} \quad (9)$$

where $Sup_{w,t}$ and $Sup_{s,t}$ represent wind and solar electricity supply at hour t, respectively. $CF_{w,t}$ and $CF_{s,t}$ refer to the capacity factors of wind and solar power at hour t, respectively.

Table 1 | Key input parameters and assumptions

Model	Category	Data item / Parameters	Resolution / Assumptions	Reference
HELM	Historical meteorological data	T2 (2m temperature, K; Kelvin), Q2 (2m specific humidity, kg kg^{-1}), WSPD (surface wind speed, m s^{-1}), SWDOWN (shortwave radiation, W m^{-2}), and GLW (longwave radiation, W m^{-2})	Hourly, 0.25° × 0.25°	[31]
	Future meteorological data	tas (air temperature), huss (specific humidity), uas/vas (wind components), rsds (shortwave radiation), and rlds (longwave radiation)	3-hourly, 50km	[32]
	Historical socioeconomic data	GDP, population	Provincial	[34][35]
	Future socioeconomic data	GDP, population	Provincial	[28][36][37]
Simulation model for net-zero power	Installed capacity	Wind, PV installed capacity	Provincial	[28][42]
	Capacity factor	Wind, PV capacity factor	Hourly, Provincial	[38][39][40]
	Energy storage	Round-trip efficiency / Self-discharge	90% / 1.14 × 10^{-}	[30]

system			^{6} per hour	
	Wind power	Cut-in / Cut-out wind speed	3 m/s / 25 m/s	[38]
	Solar PV	System efficiency / Temp. coefficient	0.85 / $-0.005\ °C^{-1}$	[39][40]

3. Scenario design

We developed four scenarios along three dimensions, reflecting varying socioeconomic developments, radiative forcing levels, and carbon neutrality timelines. All power system simulations and system adequacy assessments in this study were conducted for the target year 2060, in line with China's carbon neutrality goal. Specifically, SSP126 and SSP245 were selected as representative SSP-RCP pathways to represent different socioeconomic and climate forcing conditions [42]. To capture low-carbon transitions, we further designed the CN60 and CN50 scenario categories by imposing national carbon emission constraints to simulate provincial pathways toward carbon neutrality by 2060 and 2050, respectively. These SSP pathways were combined with CN60 and CN50 to form four combined scenarios. To assess the performance over the full 8760-hour simulation period, each scenario was evaluated under various combinations of storage duration (0-12 hours) and transmission expansion (1-4 times the reference capacity). The baseline case is defined as the reference transmission capacity without storage deployment.

Table 2 | Scenario design

Scenarios	Description	Transmission expansion levels	Storage durations
SSP126-CN60	Based on a low-emission sustainable development scenario with carbon neutrality in 2060.	1-4 times the reference capacity	0-12 hours
SSP126-CN50	Based on a low-emission sustainable development scenario with carbon neutrality in 2050.		
SSP245-CN60	Based on a medium-emission and medium sustainable development scenario with carbon neutrality in 2060.		
SSP245-CN50	Based on a medium-emission and medium sustainable development scenario with carbon neutrality in 2050.		

The results from SSP126-CN60 are presented in the main text. Results from other scenarios are available in the Supplementary Information.

4. Results

This section reports the main results of the study, progressing from electricity load forecasting and demand characteristics to system adequacy challenges and corresponding enhancement measures in a net-zero power system.

4.1 Load forecasting performance and feature importance

The HELM achieves high accuracy as measured by evaluation metrics (test MAE = 2.79, MSE = 16.68, RMSE = 4.08, $R^2 > 0.96$). Given that the tight clustering of data points around the fit line in

the predicted-actual correlation plot and the sharp, symmetric, zero-centered error distribution (Fig. 2a-b), the model demonstrates high predictive power and excellent performance. This model does not directly extrapolate in time, but rather learns the functional relationship between electricity load and its driving factors from historical data. By inputting projected future variables, the model estimates the electricity load under those conditions.

The average electricity load is primarily influenced by socioeconomic factors, while meteorological and temporal variables modulate its patterns across regions and seasons (Fig. 2c-d). The SHAP value for GDP indicates that higher absolute GDP leads to increased predicted electricity load relative to the baseline. Provinces with smaller populations generally exhibit lower electricity loads. In addition to these socioeconomic factors, the region code variable further captures interprovincial differences in industrial structure and electricity usage patterns, and thus also shows a significant influence. Regarding meteorological variables, both extremely high and low humidity exert a positive effect on electricity load. High humidity limits the body's ability to dissipate heat through evaporation, especially under hot conditions, increasing space cooling demand in residential and commercial buildings [43]. Conversely, dry winter air accelerates moisture evaporation from the skin, lowering perceived indoor temperatures and increasing heating demand. Temperature significantly increases load under extremely high or low conditions, primarily due to the use of temperature-regulating appliances such as air conditioners and electric heaters. Studies on China's southern power grid indicate that electricity consumption rises markedly above a "sensitive temperature" of around 25 °C (298.15 K) in summer and below 10 °C (283.15 K) in winter [44], while studies on Spain show that daily electricity demand has a non-linear "U-shaped" relationship with the observed mean temperature, reaching a minimum load value around 17 °C (290.15 K) [45], consistent with our model results. For solar and wind variables, higher shortwave solar radiation reduces load by decreasing daytime lighting demand, whereas the wind speed and longwave radiation contribute marginally, mainly helping capture seasonal variability [18]. Finally, temporal features reflect cyclical intra-day and seasonal patterns, as indicated by the separation between low and high feature values, which correspond to negative and positive load impacts, respectively.

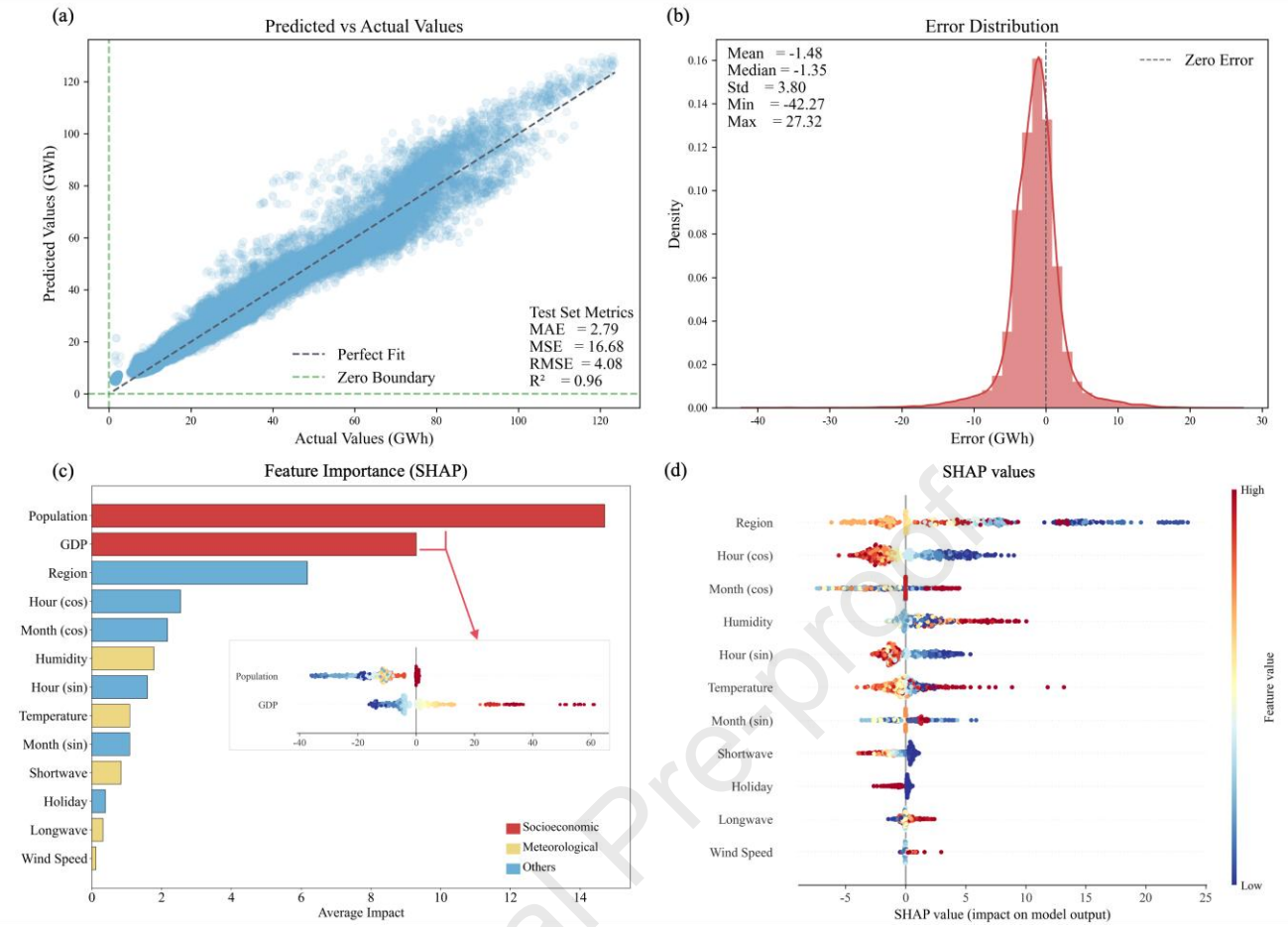

Fig. 2 | Performance and feature importance analysis of HELM. (a) predicted-actual correlation; (b) error distribution histogram; (c) feature importance ranking, illustrating the overall magnitude of each feature's impact; (d) SHAP values based on the 2060 forecasts, where the horizontal position shows the direction and magnitude of influence, and the color reflects the feature value.

4.2 Future electricity load levels and patterns

Using HELM, we forecasted hourly electricity load for 31 provinces and aggregated to estimate national demand in 2030 and 2060. The load duration curve presents all 8760 hourly values in descending order (Fig. 3a), illustrating the duration for which a given load level is met or exceeded. Results show that national demand will rise to 12100.01 TWh by 2030 and further increase to 23262.59 TWh by 2060, representing a marked increase compared with the 9852.10 TWh consumed in 2024 [2]. Expansion of power generation will be necessary to meet the growing demand, primarily through renewable energy sources.

Alongside this rapid overall growth, peak load increases are also significant. In recent years, national peak loads repeatedly set new records [46]. Model results indicate that peak load in July 2030 will reach 1804.56 GW. By July 2060, peak load is forecasted to grow to 3234.21 GW, more than double the level in 2025. The annual daily maximum and minimum load curves illustrate that China's annual load exhibits a typical dual-peak pattern, with the summer peak significantly higher than the winter peak (Fig. 3b). The increase in peak load intensifies the supply-demand gap, and

when combined with the variability of wind and solar generation, it underscores the growing need for peaking power, energy storage, and transmission to maintain reliable grid operation.

Provincial electricity loads in China are projected to increase in both magnitude and variability, reflecting differences in socioeconomic and meteorological factors. Fig. 3c-f includes the annual daily maximum and minimum load curves for Beijing, Qinghai, Jiangsu, and Fujian, which represent a range of socioeconomic and meteorological conditions in China: Beijing as a densely populated metropolis in a cold climate zone, Qinghai as a sparsely populated province with abundant renewable resources in a severe-cold zone, Jiangsu as an industrially intensive and high-load province in a hot-summer and cold-winter zone, and Fujian as a coastal region with moderate population and industrial activity in a hot-summer and warm-winter zone. The variation in absolute levels and growth rate primarily reflects differences in locational attributes and industrial structures, while load fluctuations are mainly driven by variations in residential behavioral patterns. In terms of absolute load levels, Jiangsu has the highest values, followed by Fujian, Beijing, and Qinghai. All provinces exhibit clear seasonal trends with dual summer-winter peaks, and the intraday peak-to-trough gap widens from 2030 to 2060. By 2060, the summer peak loads will reach 268.57 GW in Jiangsu, 176.47 GW in Fujian, and 81.63 GW in Beijing. Qinghai is an exception, with annual peaks of 54.67 GW occurring in winter, primarily due to heating demand driven by severe cold. Compared to Jiangsu and Beijing, Fujian's load variations are more moderate due to its milder winter climate. Overall, by 2060, both absolute load levels and fluctuations are projected to increase substantially nationwide and regionally, highlighting the significant challenges for future power system capacity planning and safe operation.

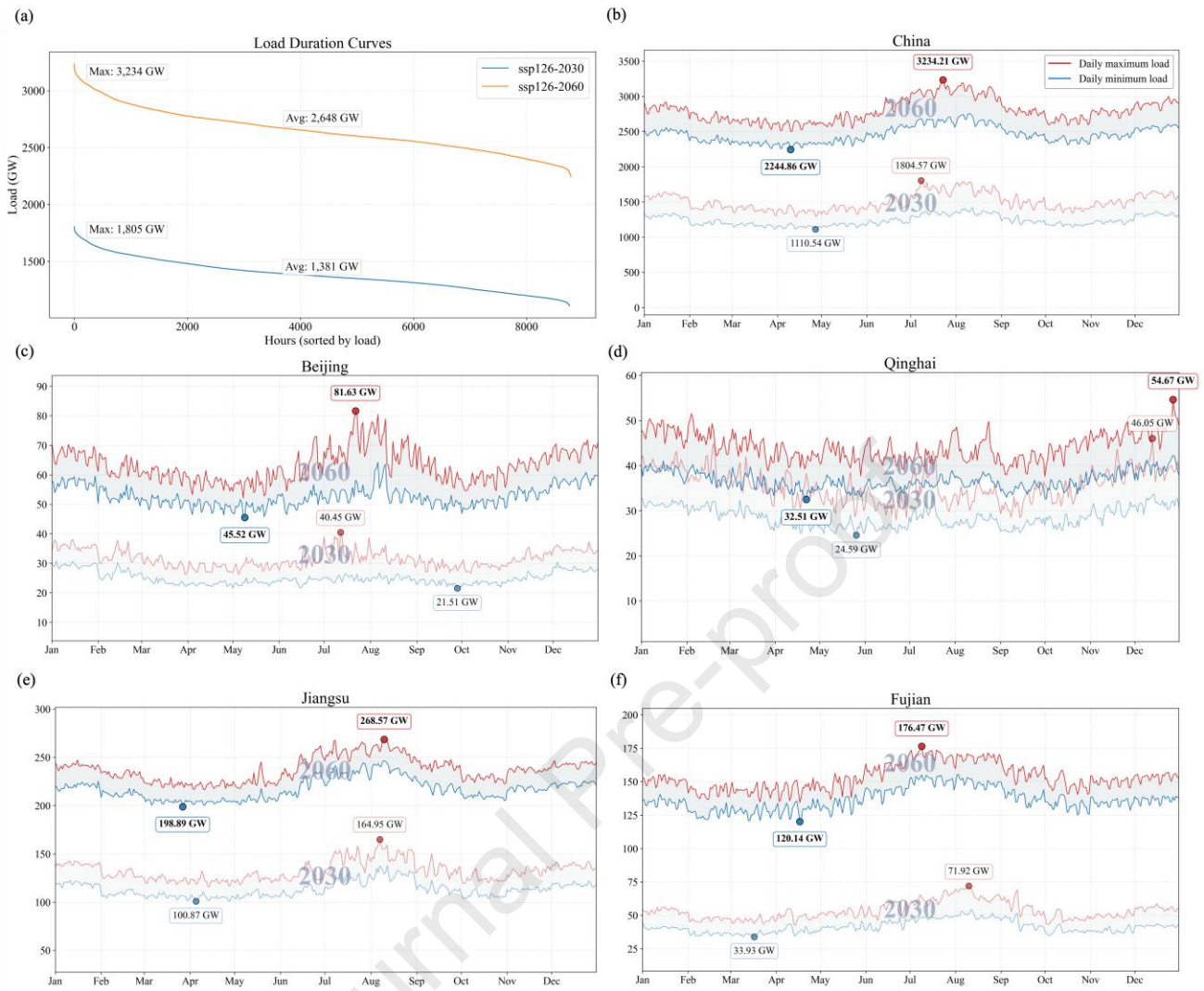

Fig. 3 | National load duration curves and daily maximum and minimum load curves under the SSP126 scenario for 2030 and 2060. (a) Load Duration Curves (LDC). (b-f) Daily maximum and minimum load curves. (b) China (national level); (c) Beijing; (d) Qinghai; (e) Jiangsu; (f) Fujian.

4.3 Electricity load response to high temperature

Although SHAP analysis does not rank temperature as the top contributor (Fig. 2c), electricity load in 2060 tends to increase markedly with rising temperature during hot summer days in 31 provinces (Fig. 4). In terms of correlation strength, 27 out of 31 provinces show an R^2 value above 0.80, with Hebei, Tianjin, and Hunan exceeding 0.98, highlighting their load sensitivity to temperature. Some regions exhibited relatively weaker fitting effects, such as Yunnan (0.76) and Hainan (0.70), suggesting that local climate conditions limit load sensitivity and that other factors influence load fluctuations. Regarding sensitivity, Shanghai (3.51 GW/K) demonstrated extremely high load sensitivity to high temperatures, likely due to its hot and humid subtropical monsoon climate combined with high air-conditioning penetration. In contrast, regions at higher latitudes or elevations, such as Heilongjiang (0.29 GW/K) and Tibet (0.11 GW/K), experience milder summers and lower cooling demand, resulting in lower sensitivity.

Our analysis of load response to high temperatures indicates that climate warming will further amplify this effect. Given the projected increase in heatwaves [47] and consequent extreme demand [45], our results lead to the conclusion that climate change will amplify the temperature-load relationship, thereby increasing the risk of extreme demand events. This highlights the urgency of incorporating climate resilience into the planning and dispatch of future net-zero power systems.

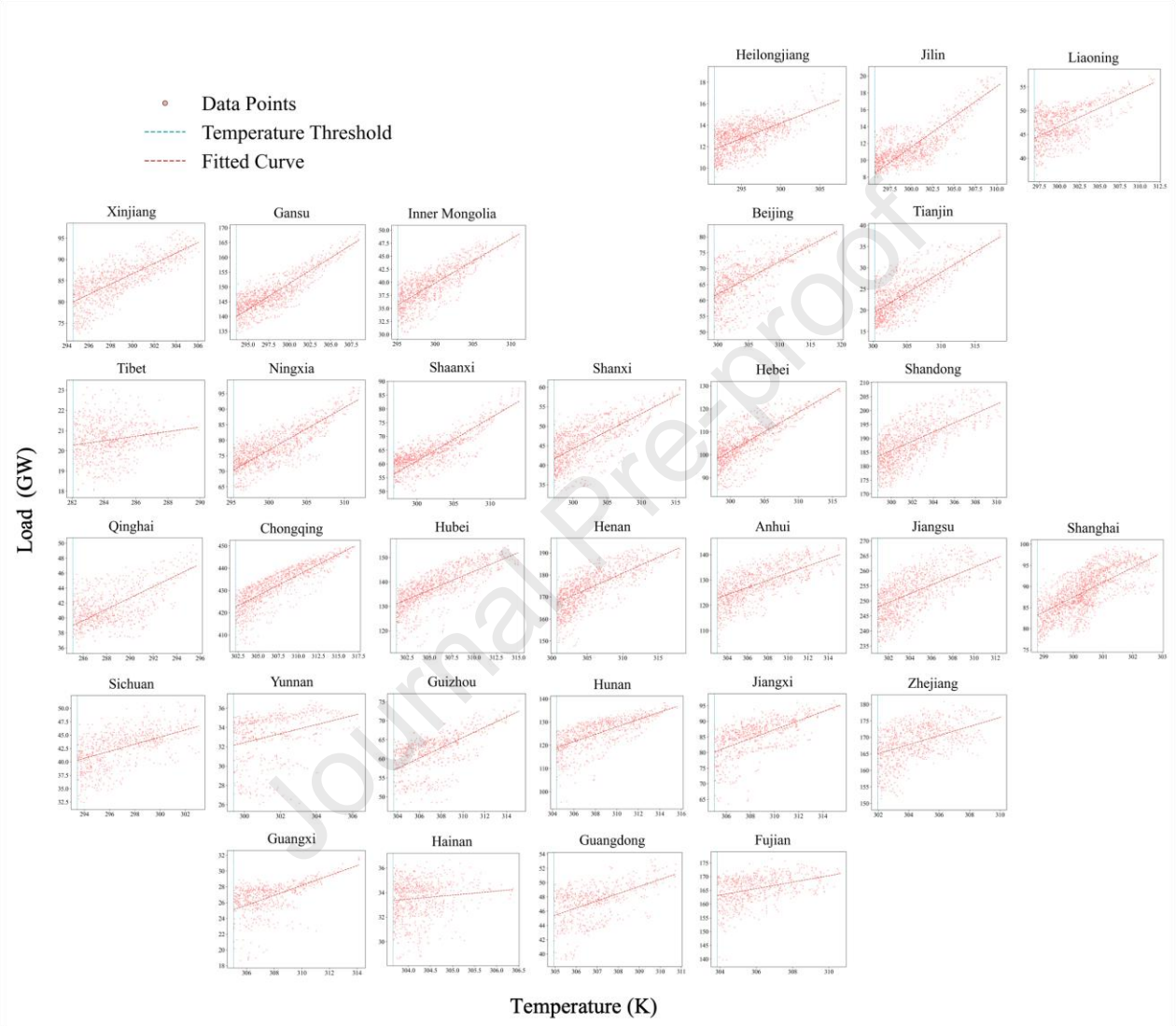

Fig. 4 | Provincial load responses to high temperature under the SSP126 scenario for 2060. Temperature data were processed in 0.5K bins to calculate the average load within each temperature interval. Results for other scenarios, along with the fitted information for each province depicted, are available in the Supplementary Information.

4.4 Challenges in net-zero power system adequacy

China's current power system exhibits significant disparities in renewable resource endowment, load distribution, and system flexibility, which shape the starting conditions for provincial transitions toward a 2060 net-zero system. Currently, provinces in the Northwest and Northeast, such as Xinjiang and Inner Mongolia, possess approximately 76% of the nation's onshore wind and solar

technical potential [48]; with relatively low local demand, these regions serve as pivotal power-exporting bases. In contrast, the eastern and central coastal regions, including the Beijing-Tianjin-Hebei, Yangtze River Delta, and Pearl River Delta clusters, account for 60%-70% of national consumption [49] while remaining persistent net importers, requiring expanded power inflows and flexible resources to ensure supply-demand balance [50]. Southwest China, led by Sichuan and Yunnan, acts as a crucial flexibility hub due to its concentrated hydropower and pumped-storage capacity [51]. In addition, several northern and central provinces, such as Shanxi and Shaanxi, currently characterized by coal-dominated generation structures, face substantial structural transitions under a net-zero pathway.

China's 30 provinces (excluding Tibet) are projected to generate 16399.14 TWh of wind and solar power by 2060 under the SSP126-CN60 scenario, and electricity demand will reach 23093.69 TWh, about 1.41 times the wind and solar generation capacity. When annual generation potential is assessed at the provincial level, without considering interprovincial transmission or energy storage, significant mismatches appear. By 2060, 11 of 30 provinces will have wind and solar generation exceeding local demand, with supply-demand ratios ranging from 1.00 to 13.40. We define these as power-exporting provinces. The remaining 19 provinces will face shortages, with ratios from 0.01 to 0.71, and are defined as power-importing provinces. Some provinces, such as Jiangsu and Henan, have large electricity demand but limited wind and solar resources; therefore, over 90% of their electricity demand cannot be met by local renewable generation. In contrast, Xinjiang, Inner Mongolia, and Gansu have the highest wind and solar potential, collectively accounting for 48.36% of the nation's generation (Fig. S4), while electricity consumption accounts for only 9.58% of the national total, resulting in a significant surplus.

Under the baseline case with the reference transmission capacity and without energy storage, the national annual adequacy stands at 57.56% (Fig. S5), indicating the percentage of hours in which electricity load can be met by wind and solar power. The national annual deficit falls to 8934.35 TWh, and 8077.14 TWh to annual curtailment. Power-exporting provinces in northern and western China, such as Inner Mongolia, Xinjiang, Heilongjiang, Jilin, produce at least four times their local load from wind and solar, with adequacy exceeding 93% (Fig. 5). However, they face severe curtailment, including 4058.71 TWh in Inner Mongolia and 1117.99 TWh in Xinjiang (Fig. 6b). Other power-exporting provinces, such as Ningxia, Gansu, and Yunnan, also exceed local demand. Still, their adequacy remains between 50% and 80%, with curtailment volumes from 127.35 TWh to 663.07 TWh. Power shortages occur during peak load periods, while surplus generation during low-load periods cannot be fully utilized. Remarkably, Beijing, Tianjin, Shanghai, and Shandong have very low supply-demand ratios, with Beijing's ratio being just 0.05. Yet their adequacy still exceeds 90%, with Beijing and Tianjin reaching 99.42% and 99.91%, respectively. These provinces rely heavily on imports, with annual inflows from 144.65 TWh to 689.69 TWh, mainly from Inner Mongolia and Hebei (Fig. 7). Other power-importing provinces in the east and south exhibit power adequacy below 80% under the baseline case, with Fujian, Chongqing, and Hainan even falling below 20%, experiencing substantial unserved energy (Fig. 6a).

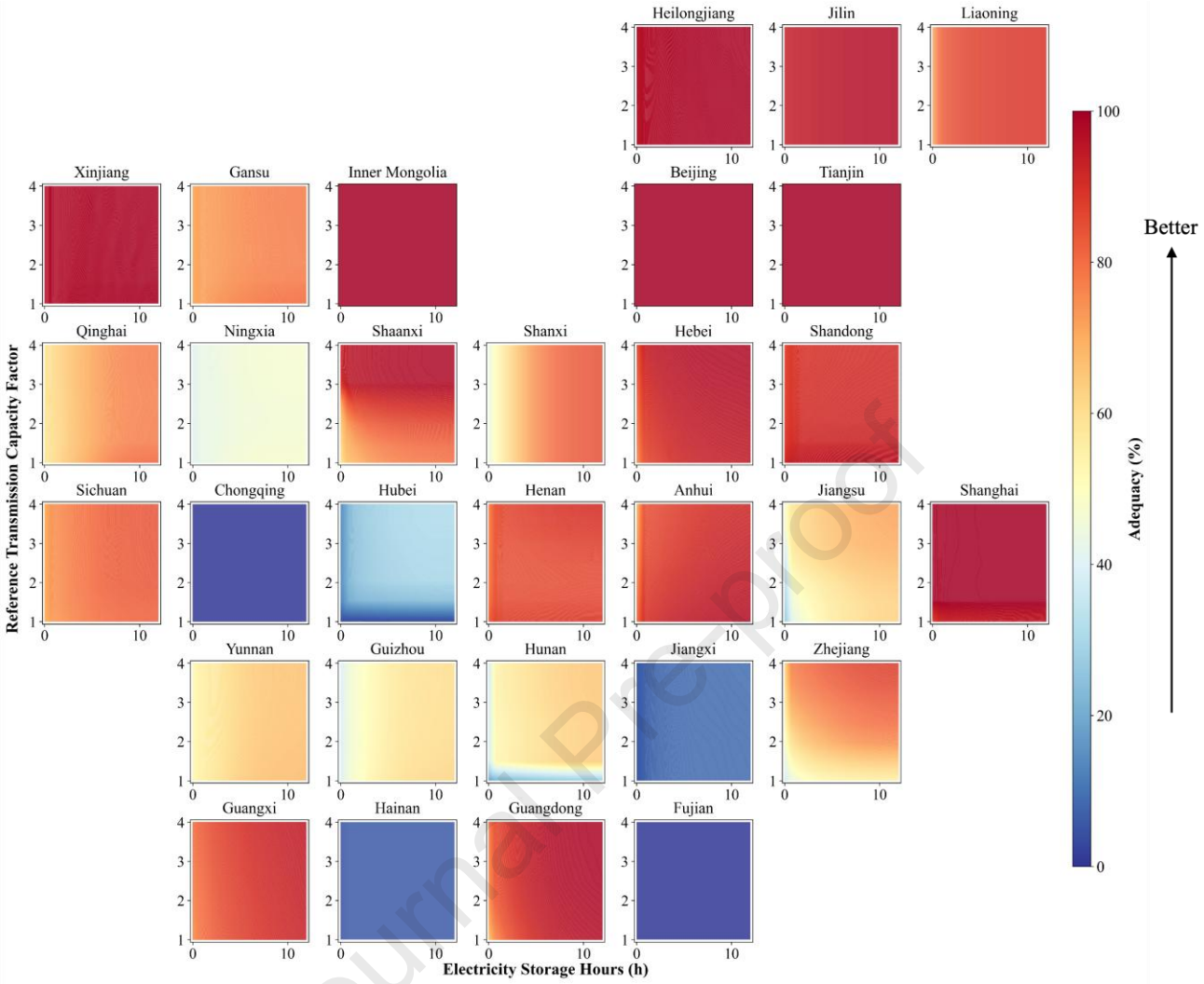

Fig. 5 | Provincial net-zero power system adequacy under the SSP126-CN60 scenario for 2060. Adequacy is presented as a function of energy storage duration (x-axis, 0-12 hours) and relative interprovincial transmission capacity factor (y-axis, 1-4 times the reference transmission capacity). Colors indicate adequacy, ranging from 0% (blue) to 100% (dark red). Results for other scenarios and national-scale plots are available in the Supplementary Information.

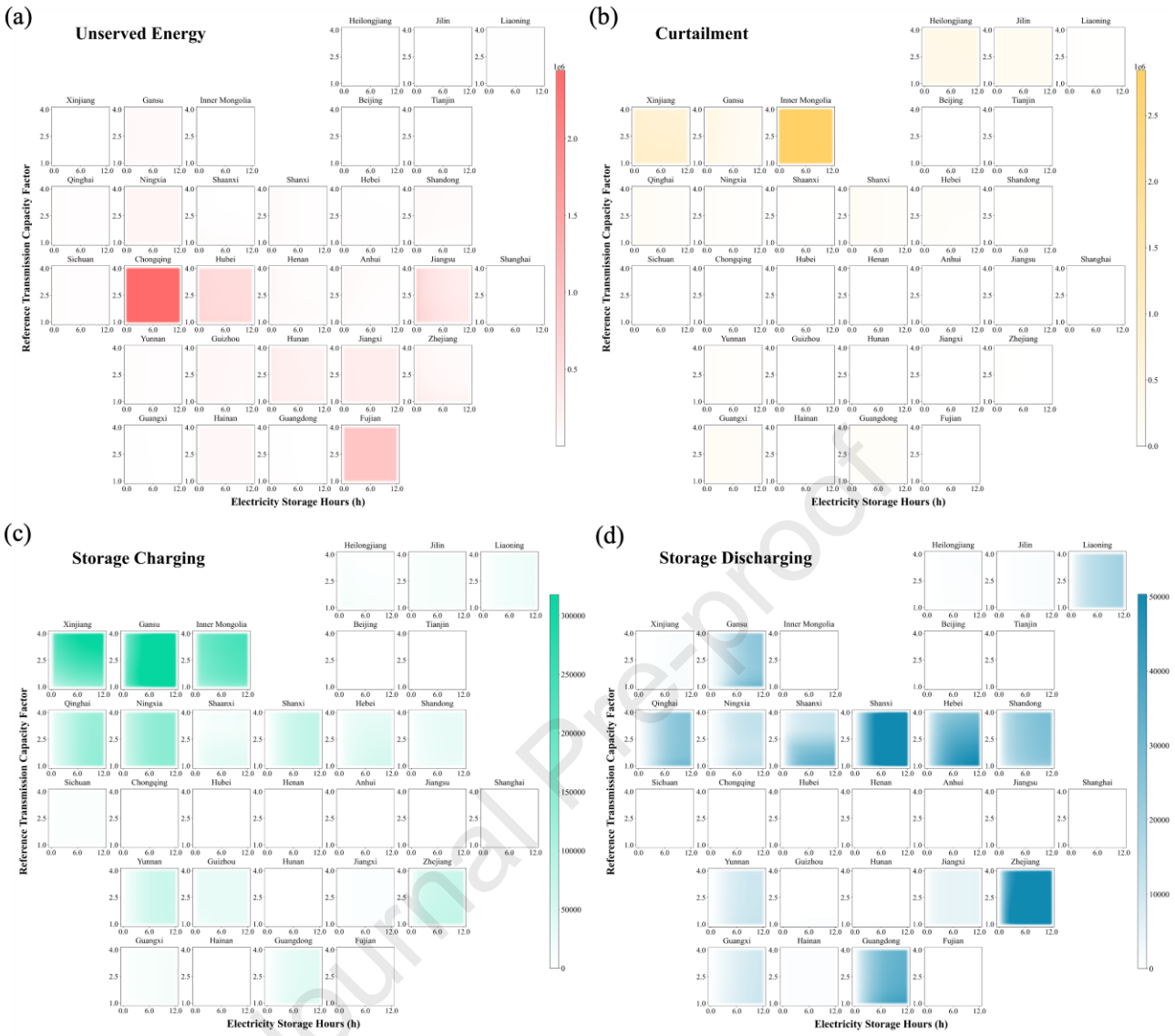

Fig. 6 | Key performance metrics for provincial net-zero power system under the SSP126-CN60 scenario for 2060. Metrics are shown as a function of energy storage duration (x-axis, 0-12 hours) and relative interprovincial transmission capacity factor (y-axis, 1-4 times the reference transmission capacity). Grid-side energy storage maintains an annual SOC balance at the national level. (a) annual unserved energy (GWh); (b) annual curtailment (GWh); (c) annual storage charging (GWh); (d) annual storage discharging (GWh). Results for other scenarios are available in the Supplementary Information.

4.5 Enhancements in net-zero power system adequacy

Transmission and energy storage are essential for addressing the spatiotemporal mismatch of wind and solar power. Interprovincial transmission helps balance regional differences in renewable generation by utilizing complementary resources, diverse geographies, and varying weather patterns. By 2024, China's interprovincial transmission infrastructure capacity exceeded 300 GW, supported by 40 ultra-high voltage (UHV) lines totaling about 54000 km [52]. In 2060, at the national level and without energy storage, utilizing the reference transmission capacity enables 4486.18 TWh of national transfers, achieving an adequacy of 57.56%. When transmission capacity increases from 1 to

3 times the reference level, adequacy rises to 61.19%. Energy storage technologies such as flow, lithium-ion, and compressed air systems mitigate the intermittency of wind and solar power [53]. Despite challenges in cost and scalability, energy storage remains essential for system flexibility [54]. Under reference transmission capacity, a 6-hour storage increase raises national adequacy to 67.84%, while a 12-hour storage increase further increases it to 69.63% (Fig. S5).

At the provincial level, expanding transmission and storage can ease challenges in both power-exporting and power-importing provinces (Fig. 5). In power-importing provinces, electricity deficits are reduced through two mechanisms. First, power imports from power-exporting provinces increase as transmission expands (Fig. 7). For instance, when transmission capacity is increased from 1 to 3 times the reference level with 3-hour storage, Zhejiang's imports rise by 64.72 TWh, and adequacy improves from 50.56% to 75.87%. Jiangsu's imports increase by 192.80 TWh, with adequacy rising from 50.26% to 62.90%. Second, local storage supplements supply during peak periods (Fig. 6d). Provinces with high energy storage discharge volumes highly overlap with regions experiencing severe power shortages, highlighting the critical role of energy storage in enhancing local power sufficiency. Under a reference transmission capacity, extending storage from 0 to 12 hours boosts Zhejiang's discharge by 66.22 TWh, raising adequacy from 36.13% to 54.60%. In power-exporting provinces, greater transmission and storage help reduce curtailment. Extra transmission allows more direct exports of surplus power (Fig. 7). At the same time, additional storage enables local absorption of excess generation (Fig. 6c). When transmission capacity increases from 1 to 3 times and 3-hour storage, Inner Mongolia's exports rise by 512.09 TWh, while curtailment decreases by 64.88 TWh. Extending storage from 3 to 12 hours adds 31.01 TWh of charging, further improving the use of surplus renewables.

As the capacities of transmission and energy storage increase, they demonstrate a complementary relationship—enhancements in one can partly substitute for the other, while coordinated expansion can further improve overall system adequacy. Specifically, the transmission saturation point drops from 3.5 to 3.0 times when storage exceeds 3.75 hours (Fig. S6), while the storage saturation point decreases from 7.5 to 6.75 hours when transmission exceeds 2.5 times (Fig. S7) for national adequacy. National adequacy exceeds 70% with 1.6 times transmission and 6-hour storage, or with 3.5 times transmission and 3.7-hour storage (Fig. S5). Beyond these levels, further expansion yields diminishing returns, suggesting an efficient configuration range of 2-3 times transmission and 4-5 hours storage.

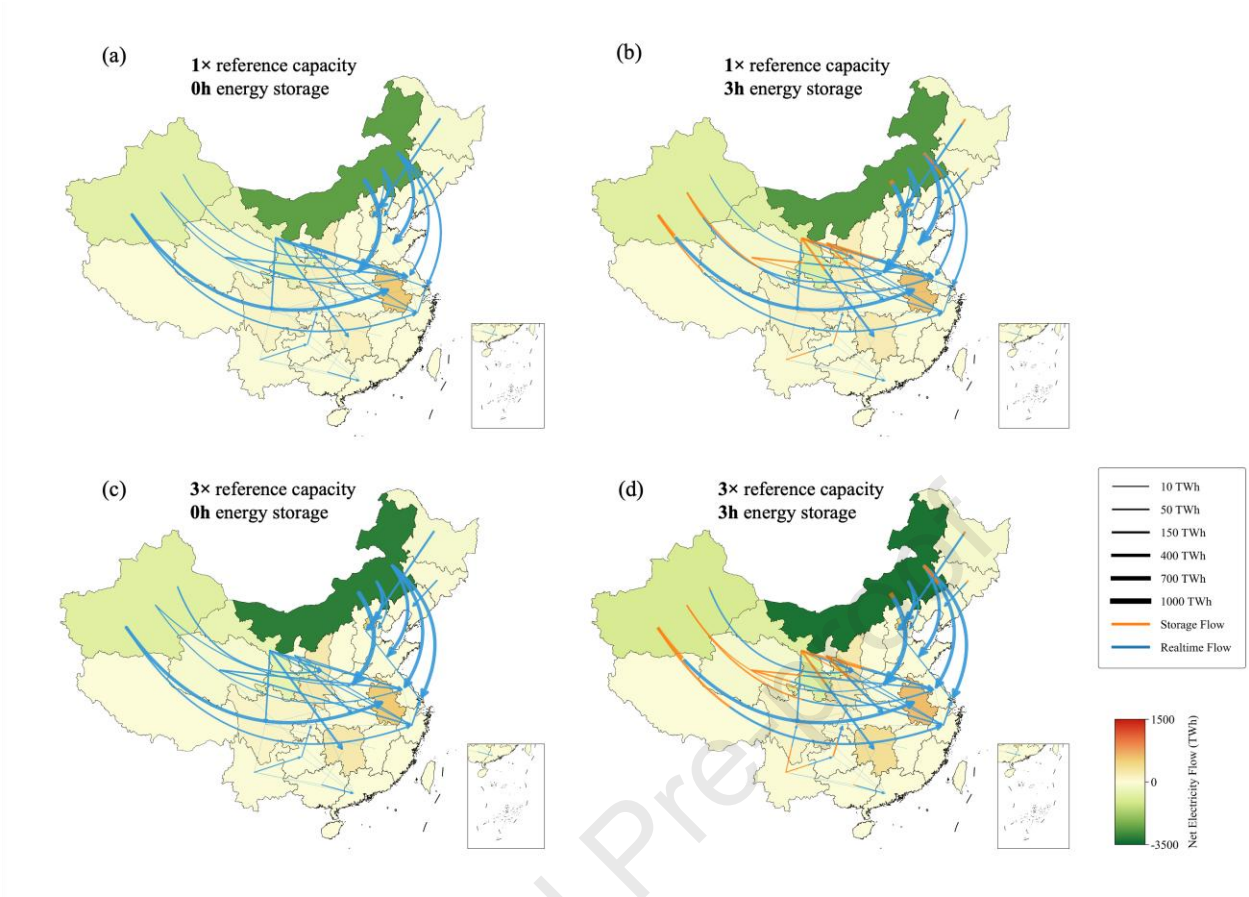

Fig. 7 | Interprovincial electricity transmission under the SSP126-CN60 scenario for 2060. Net electricity flow is the total electricity flowing into the province minus the total electricity flowing out of the province. Real-time flow refers to direct real-time power transmission between provinces, while storage flow represents electricity transferred via storage discharge. Panels correspond to combinations of transmission capacity and energy storage duration: (a) 1×, 0h; (b) 1×, 3h; (c) 3×, 0h; (d) 3×, 3h. Results for other scenarios are available in the Supplementary Information.

At intra-day and inter-day scales, Fig. 8 shows the electricity load and supply in Inner Mongolia and Zhejiang using 2 times the reference transmission capacity and 3-hour storage. Such patterns highlight that transmission plays a crucial role in cross-regional support, while storage helps with peak shaving and valley filling. As a power-exporting province, Inner Mongolia's wind and solar generation far exceeds local load, with daily output reaching 6-10 times provincial needs. Summer output is generally higher than winter, with peak summer daily generation of 17901.19 GWh. Winter storage charging volumes are higher, reaching a single-day maximum of 855.59 GWh. This is mainly because electricity demand in importing provinces declines during winter, which lowers transmission and increases the potential for storage. As a power-importing province, Zhejiang's wind and solar generation can meet about 8 consecutive hours of load on a typical summer day. During the daytime, rising solar output first supports local self-sufficiency, then enables power exports, and eventually facilitates the charging of storage systems. By 16:00 or even earlier in winter, local wind and solar generation often fall short of the load, resulting in a peak summer deficit of up to 122.76

GW. After this time, power imports and storage discharge begin to supplement supply, with storage progressively substituting for solar as its output approaches zero by 18:00. Expanding transmission capacity or storage duration further increases their contribution. Annual adequacy improves from 36.13% with reference transmission and no storage to 87.94% with 4 times transmission and 12-hour storage (Fig. S20). Seasonal differences are also evident. In July, Zhejiang's daily solar generation is roughly 2-6 times higher than in January, resulting in much larger charging and discharging volumes in summer. In winter, although solar generation declines, renewables can cover about 3 hours of local load on a typical winter day. Winter imports rise substantially, with daily transmission volumes 2-5 times higher than in summer.

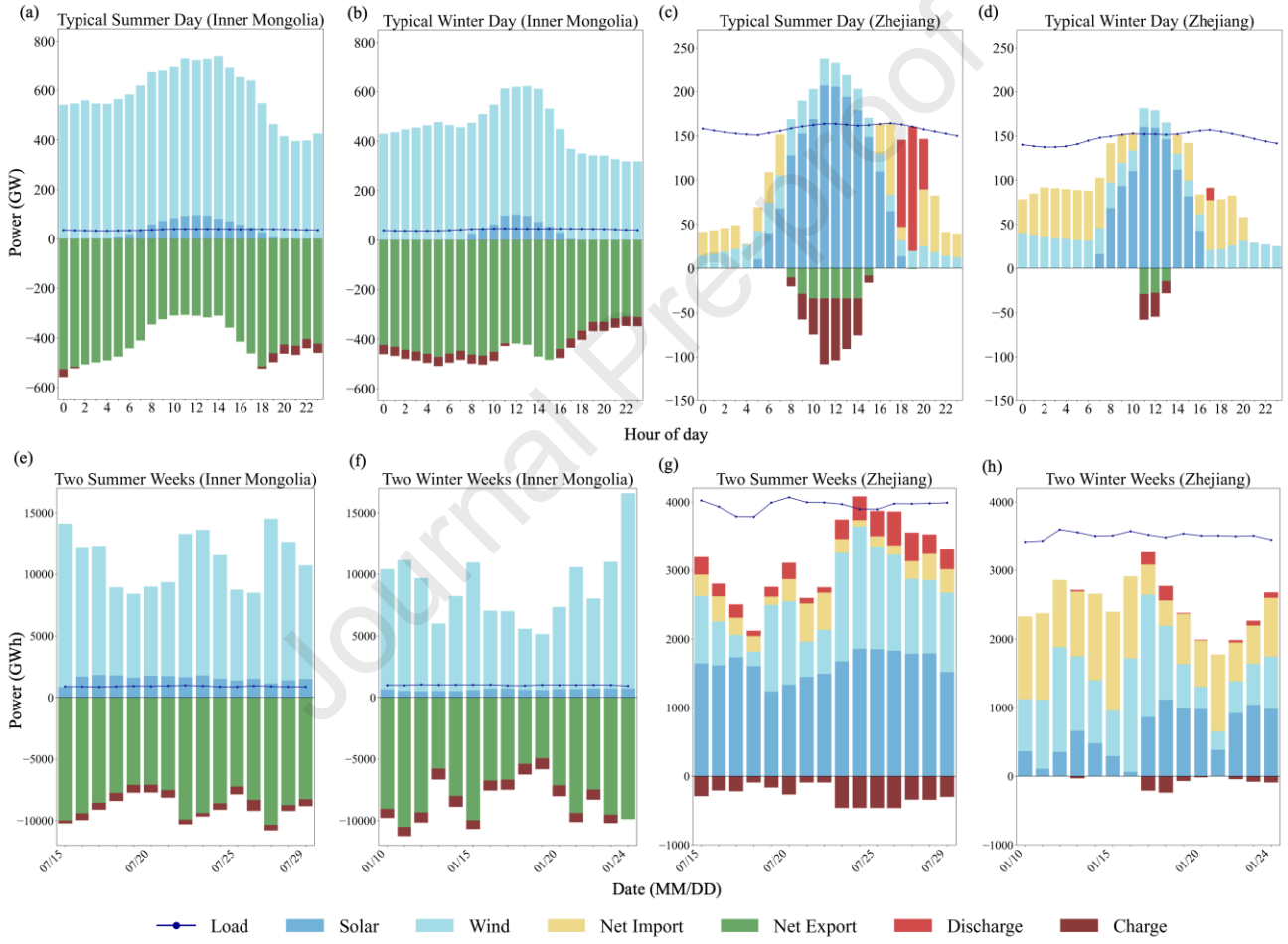

Fig. 8 | Electricity load and supply in Inner Mongolia and Zhejiang with 2 times the reference transmission capacity and 3-hour storage for 2060. (a-b) typical summer and winter day in Inner Mongolia; (c-d) typical summer and winter day in Zhejiang; (e-f) biweekly load and supply in summer and winter in Inner Mongolia; (g) biweekly load and supply in summer and winter in Zhejiang.

5. Discussion

Our analysis indicates that China's electricity demand is forecasted to grow rapidly under future socioeconomic and climate conditions, more than doubling between 2024 (9852 TWh) and 2060

(23262 TWh), and exhibiting peak patterns in summer and winter. Socioeconomic variables dominate long-term load growth, while temperature significantly increases load under extreme heat and cold, emerging as a critical driver during hot summers and reflecting the amplifying effect of climate change. These findings on load levels and patterns highlight the challenges that future power systems are likely to encounter on the demand side.

Power systems dominated by wind and solar will face significant spatiotemporal mismatches between generation and load in 2060. In the baseline case under SSP126-CN60, the adequacy of the national net-zero power system falls to 57.6%. Provinces such as Beijing and Tianjin, where local wind and solar generation is insufficient to meet demand, still achieve over 99% adequacy by relying on imports from regions like Inner Mongolia and Hebei. Conversely, resource-rich provinces such as Qinghai and Gansu face adequacy risks of only 50-80% due to diurnal and seasonal variability. This highlights that even power-exporting provinces must develop robust local flexibility. Achieving a fully renewable electricity system depends on integrated planning of flexible resources, refined dispatch strategies, and strengthened regional coordination.

Interprovincial transmission addresses spatial mismatches in power systems. It enables large-scale power transfers, such as the “West-to-East Power Transmission,” to address geographical imbalances, while also leveraging time-zone differences and varying demand patterns. Energy storage alleviates temporal mismatches through peak shaving and valley filling, enhancing local grid flexibility and real-time balancing to support the reliable integration of renewable energy. Together, they provide complementary flexibility that enhances system adequacy and reduces curtailment at both national and provincial levels and across annual, intra-day, and inter-day timescales. A configuration with 2-3 times the reference transmission capacity and 4-5 hours of storage achieves over 70% adequacy, beyond which further expansion yields diminishing marginal improvements.

Even with substantial expansion of transmission and storage, a residual adequacy gap persists. Addressing the remaining adequacy gap requires the introduction of firm and flexible resources. Firm capacity sources, such as nuclear power and CCS-equipped thermal units, provide stable output during prolonged periods of low renewable generation. Flexible resources, including reservoir-based hydropower, support seasonal and intraseasonal regulation through dispatchable operation. These options involve system-level trade-offs. CCS incurs efficiency penalties and higher costs, while nuclear power and large hydropower are constrained by resource availability and environmental considerations.

These findings offer clear implications for China’s dual carbon strategy. First, differentiated development strategies for wind and solar are needed. Based on technological maturity and regional resource endowments, promote distributed photovoltaics and onshore wind power by optimizing market and grid connection standards, while providing targeted support for offshore wind and concentrated solar power. Second, interprovincial transmission planning should be strengthened to alleviate corridor constraints and enhance national coordination, with priority given to key west-to-east transmission routes to facilitate large-scale renewable integration (e.g., Inner Mongolia-Jiangsu and Xinjiang-Zhejiang). Third, establishing a capacity value compensation mechanism for energy

storage is essential to incentivize investment and recognize its reliability contribution. Finally, strategic deployment of storage hubs in both renewable-rich regions and major load centers, supported by interprovincial cost-sharing mechanisms, would improve corridor utilization and enhance system-wide stability.

Overall, this study establishes an integrated assessment framework to analyze how an adequate net-zero power system can be achieved under climate change, providing valuable quantitative insights for China's future energy transition pathway. Methodologically, it advances high-resolution forecasting and system-level assessment by integrating socioeconomic and meteorological factors within a neural network framework to generate long-term, province-level hourly forecasts. The framework further links climate-sensitive load, variable renewable generation, transmission, and storage, enabling supply-demand evaluation across transition scenarios. This approach provides analytical support for renewable integration and regional power planning in China, while offering transferable tools for long-term energy transition analysis in other regions.

Although this study presents a comprehensive framework, several limitations remain. The analysis relies on a simulation-based framework rather than optimization. Most existing studies rely on 8760-hour provincial cost-optimization models that aggregate the national system, simplify interprovincial transmission, or apply temporal clustering to address computational constraints, which may underestimate renewable variability and introduce bias. Our study focuses on evaluating the adequacy of a wind-solar-storage system under future climate change rather than identifying a cost-optimal pathway. A high-resolution simulation framework enables explicit representation of resources while avoiding distortions. In addition, nighttime light data are excluded from HELM due to the lack of future projections and their strong correlation with population and GDP.

Future work could incorporate economic considerations to jointly assess overall system performance, while also exploring a broader portfolio of low-carbon and flexibility-enhancing technologies to support a reliable net-zero transition.

CRediT authorship contribution statement

Jinning Lyu: Writing - original draft, Visualization, Software, Methodology, Investigation, Formal analysis, Data curation, Conceptualization. **Jinhui Ren:** Writing - review & editing, Validation, Methodology, Investigation, Formal analysis, Conceptualization. **Shu Zhang:** Writing - review & editing, Supervision, Conceptualization. **Wenying Chen:** Writing - review & editing, Validation, Supervision, Resources, Conceptualization.

Declaration of competing interests

The authors declare that they have no known competing financial interests or personal relationships that could have appeared to influence the work reported in this paper.

Data availability

Data will be made available on request.

Acknowledgments

This study was supported by the National Science and Technology Major Project of the Ministry of Science and Technology of China (2024ZD1406606), Ministry of Education Project of Key Research Institute of Humanities and Social Sciences at Universities (22JJD480001), and the National Natural Science Foundation of China (72504162).

Additional information

Refer to the Supplementary Information file.

References

[1] Muttitt G, Price J, Pye S, et al., 2023. Socio-political feasibility of coal power phase-out and its role in mitigation pathways. Nat. Clim. Change 13, 140-147. https://doi.org/10.1038/s41558-022-01576-2.

[2] National Energy Administration, 2025. Total electricity consumption across society increased by 6.8% year-on-year in 2024. https://www.nea.gov.cn/20250120/4f7f249bac714e7693adecac996d742f/c.html [2025-08-30].

[3] Qiu, L., Khorramfar, R., Amin, S., Howland, M.F., 2024. Decarbonized energy system planning with high-resolution spatial representation of renewables lowers cost. Cell Reports Sustainability 1, 100263. https://doi.org/10.1016/j.crsus.2024.100263.

[4] Zhuo, Z. et al., 2022. Cost increase in the electricity supply to achieve carbon neutrality in China. Nat. Commun. 13, 3172. https://doi.org/10.1038/s41467-022-30747-0.

[5] Mongird K., Burledyson C., Akdemir K. Z., Rice J., 2023. Electric grid visualization: hourly renewable generation, load, unserved load, and locational marginal prices during a heatwave. Pacific Northwest National Laboratory (PNNL), Richland, WA. https://doi.org/10.57931/2001010.

[6] Xu, L., Feng, K., Lin, N. et al, 2024. Resilience of renewable power systems under climate risks. Nat Rev Electr Eng 1, 53–66. https://doi.org/10.1038/s44287-023-00003-8

[7] Deroubaix, A. et al., 2021. Large uncertainties in trends of energy demand for heating and cooling under climate change. Nat. Commun. 12, 5197. https://doi.org/10.1038/s41467-021-25504-8.

[8] Clack, C. T. M. et al., 2017. Evaluation of a proposal for reliable low-cost grid power with 100% wind, water, and solar. Proc. Natl Acad. Sci. USA 114, 6722 – 6727. https://doi.org/10.1073/pnas.1610381114.

[9] Intergovernmental Panel on Climate Change. Climate Change 2021: The Physical Science Basis. https://www.ipcc.ch/report/ar6/wg1/ (IPCC, 2021).

[10] Zhang, S., Liao, X., Cheng, Y., 2021. Short-term electricity demand forecasting method based

on characteristic analysis and LSTM neural network. Electric Power Big Data 24(5), 9-17 (in Chinese).

[11] Alipour, P., Mukherjee, S., & Nateghi, R., 2019. Assessing climate sensitivity of peak electricity load for resilient power systems planning and operation: A study applied to the Texas region. Energy. https://doi.org/10.1016/J.ENERGY.2019.07.074.

[12] Staffell, I., Pfenninger, S., 2018. The increasing impact of weather on electricity supply and demand Energy 145 65-78. https://doi.org/10.1016/j.energy.2017.12.051.

[13] Chandrasekaran, R., Paramasivan, S.K., 2025. Advances in Deep Learning Techniques for Short-term Energy Load Forecasting Applications: A Review. Arch Computat Methods Eng 32, 663–692. https://doi.org/10.1007/s11831-024-10155-x.

[14] Thamer Mustafa, A., Al-Deen Al-Yozbaky, O.S., 2025. Forecasting energy demand and generation using time series models: A comparative analysis of classical, grey, fuzzy, and intelligent approaches. Franklin Open 100350. https://doi.org/10.1016/j.fraope.2025.100350.

[15] McGrath, C.R., Burleyson, C.D., Khan, Z., Rahman, A., Thurber, T., Vernon, C.R., Voisin, N., Rice, J.S., 2022. tell: A python package to model future total electricity loads in the United States. JOSS 7, 4472. https://doi.org/10.21105/joss.04472.

[16] Akdemir K. Z., Mongird, K., Kern, J.D., Oikonomou, K., Voisin, N., Burleyson, C.D., Rice, J.S., Zhao, M., Bracken, C., Vernon, C., 2025. Investigating the effects of cooperative transmission expansion planning on grid performance during heat waves with varying spatial scales. Applied Energy 378, 124825. https://doi.org/10.1016/j.apenergy.2024.124825

[17] Byers, E. A., Coxon, G., Freer, J., 2020. Drought and climate change impacts on cooling water shortages and electricity prices in great britain. Nature Commun. 11(1): 2239. https://doi.org/10.1038/s41467-020-16012-2.

[18] Richardson, D., Hobeichi, S., Sweet, L., Rey-Costa, E., Abramowitz, G., Pitman, A.J., 2024. Predicting Australian energy demand variability using weather data and machine learning. Environ. Res. Lett. 20, 014028. https://doi.org/10.1088/1748-9326/ad9b3b.

[19] Bloomfield, H. C., Brayshaw, D. J., Troccoli, A., 2021. Quantifying the sensitivity of european power systems to energy scenarios and climate change projections. Renewable Energy, 164: 1062-1075. https://doi.org/10.1016/j.renene.2020.09.125.

[20] Tang, B., Wu, Y., Yu, B., et al., 2025. Integrating climate change impacts into power system planning for achieving carbon neutrality in China. Structural Change and Economic Dynamics, 2025, 73: 248-261. https://doi.org/10.1016/j.strueco.2025.01.003.

[21] van Ruijven, B.J., De Cian, E., and Wing, I.S., 2019. Amplification of future energy demand growth due to climate change. Nat. Commun. 10, 2762. https://doi.org/10.1038/s41467-019-10399-3.

[22] Gernaat, D.E., de Boer, H.S., Daioglou, V., Yalew, S.G., M¨uller, C., and van Vuuren, D.P., 2021. Climate change impacts on renewable energy supply. Nat. Clim. Change 11, 119–125. https://doi.org/10.1038/s41558-020-00949-9.

[23] Zheng, D., Tong, D., Davis, S.J., Qin, Y., Liu, Y., Xu, R., Yang, J., Yan, X., Geng, G., Che, H.,

Zhang, Q., 2024. Climate change impacts on the extreme power shortage events of wind-solar supply systems worldwide during 1980-2022. Nat Commun 15, 5225. https://doi.org/10.1038/s41467-024-48966-y.

[24] Tong, D., Farnham, D.J., Duan, L., Zhang, Q., Lewis, N.S., Caldeira, K., Davis, S.J., 2021. Geophysical constraints on the reliability of solar and wind power worldwide. Nat Commun 12, 6146. https://doi.org/10.1038/s41467-021-26355-z.

[25] Zhao, Z. J., Chen, X., Ma, Z. Y., Yang, F., Zhang, H. N., 2025. Climate impacts on the supply–demand balance of China's wind–solar energy system based on power grid transmission during the summer peak-load period. Advances in Climate Change Research, Special Issue on Technological Innovation for Adaptation to Climate Change 16, 718–729. https://doi.org/10.1016/j.accre.2025.07.008

[26] Zheng, D., Yan, X., Tong, D., Davis, S.J., Caldeira, K., Lin, Y., Guo, Y., Li, J., Wang, P., Ping, L., Feng, S., Liu, Y., Cheng, J., Chen, D., He, K., Zhang, Q., 2025. Strategies for climate-resilient global wind and solar power systems. Nature 643, 1263–1270. https://doi.org/10.1038/s41586-025-09266-7.

[27] Fan, J.L., Li, Z., Huang, X., et al., 2023. A net-zero emissions strategy for China's power sector using carbon-capture utilization and storage. Nat. Commun. 14(1): 5972. https://doi.org/10.1038/s41467-023-41548-4.

[28] Zhang, Q., Zhang, S., Chen, W., 2024. Provincial pathways to carbon-neutral energy systems in China considering interprovincial electricity transmission development. Applied Energy, 2024, 375: 123953. https://doi.org/10.1016/j.apenergy.2024.123953.

[29] Ren, J., Zhang, Q., Chen, W.,2024. China's provincial power decarbonization transition in a carbon neutral vision. Energy 310, 133211. https://doi.org/10.1016/j.energy.2024.133211.

[30] Wang, H., Jiang, Y., Manthiram, A., 2018. Long cycle life, low self-discharge sodium-selenium batteries with high selenium loading and suppressed polyselenide shuttling. Adv. Energy Mater. 8, 1701953. https://doi.org/10.1002/aenm.201701953.

[31] Hersbach, H., Muñoz-Sabater, J., Bell, B., et al., 2023. ERA5 hourly data on single levels from 1940 to present [Data set]. Copernicus Climate Change Service (C3S) Climate Data Store (CDS). https://doi.org/10.24381/cds.adbb2d47.

[32] Wu, T., Lu, Y., Fang, Y., et al., 2019. The Beijing Climate Center Climate System Model (BCC-CSM): the main progress from CMIP5 to CMIP6. Geoscientific Model Development, 12(4), 1573-1600. https://doi.org/10.5194/gmd-12-1573-2019.

[33] Moghim, S., McKnight, S.L., Zhang, K., Ebtehaj, A.M., Knox, R.G., Bras, R.L., Moorcroft, P.R., Wang, J., 2017. Bias-corrected data sets of climate model outputs at uniform space–time resolution for land surface modelling over amazonia. International Journal of Climatology 37, 621–636. https://doi.org/10.1002/joc.4728.

[34] China Electricity Council. China Electricity Statistics Yearbook 2024[M]. China: China Statistics Press, 2024.

[35] China Electricity Council. China Electricity Statistics Yearbook 2023[M]. China: China Statistics Press, 2023.

[36] Yang, Y.M., Zhai, J.Q., Su, B.D., et al., 2024. National and provincial economy projection databases under Shared Socioeconomic Pathways (SSP1-5) _v2. Clim. Change Res. 20 (4), 498–503. https://doi.org/10.57760/sciencedb.01683.

[37] Guo, H. H., Jing, C., Jiang, T., et al., 2024. National and provincial population projection databases under Shared Socioeconomic Pathways (SSP1-5) _v2. Clim. Change Res. 20 (4), 492–497. https://doi.org/10.57760/sciencedb.01683.

[38] Zhao, Y., Liang, S., Liu, Y., et al., 2023. Global assessment of spatiotemporal changes of frequency of terrestrial wind speed. Environmental Research Letters; 18. https://doi.org/10.1088/1748-9326/acc9d5.

[39] Braun, J.E., Mitchell, J.C., 1983. Solar geometry for fixed and tracking surfaces. Sol. Energy 31, 439-444. https://doi.org/10.1016/0038-092X(83)90046-4.

[40] Gernaat, D. E. H. J. et al., 2021. Climate change impacts on renewable energy supply. Nat. Clim. Chang. 11, 119-125. https://doi.org/10.1038/s41558-020-00949-9.

[41] Zheng, D. et al., 2025. Strategies for climate-resilient global wind and solar power systems. Nature. https://doi.org/10.1038/s41586-025-09266-7.

[42] IPCC, 2021. Climate Change 2021: The Physical Science Basis. Contribution of Working Group I to the Sixth Assessment Report (AR6).

[43] Rastogi, D., Lehner, F., Kuruganti, T., Evans, K.J., Kurte, K., Sanyal, J., 2021. The role of humidity in determining future electricity demand in the southeastern united states. Environ. Res. Lett. 16, 114017. https://doi.org/10.1088/1748-9326/ac2fdf.

[44] Li, Y., Lin, B., Shao, C., Liu, Z., Yuan, K., Dong, N., 2024. A new method for calculating temperature-controlled load electricity consumption based on sensitive temperature detection, in: 2024 The 9th International Conference on Power and Renewable Energy (ICPRE). Presented at the 2024 The 9th International Conference on Power and Renewable Energy (ICPRE), IEEE, Guangzhou, China, pp. 1713–1717. https://doi.org/10.1109/ICPRE62586.2024.10768294.

[45] Garrido-Perez, J.M., Barriopedro, D., García-Herrera, R., Ordóñez, C., 2021. Impact of climate change on spanish electricity demand. Climatic Change 165, 50. https://doi.org/10.1007/s10584-021-03086-0

[46] China Electricity Council, 2025. Total electricity consumption across society increased by 6.8% year-on-year in 2024.

[47] K.P. Tripathy, S. Mukherjee, A.K. Mishra, M.E. Mann, & A.P. Williams, 2023. Climate change will accelerate the high-end risk of compound drought and heatwave events, Proc. Natl. Acad. Sci. U.S.A. 120 (28) e2219825120, https://doi.org/10.1073/pnas.2219825120.

[48] Tian, J., Zhou, S., & Wang, Y., 2023. Assessing the technical and economic potential of wind and solar energy in China—A provincial-scale analysis. Environmental Impact Assessment Review. https://doi.org/10.1016/j.eiar.2023.107161.

[49] Shi, X., & Zhong, Y., 2024. Research on the temporal and spatial pattern evolution characteristics

and decoupling effect of electricity power consumption in China. Sustainable Cities and Society. https://doi.org/10.1016/j.scs.2024.105558.

[50] Yao, H., & Zang, C., 2021. The spatiotemporal characteristics of electrical energy supply-demand and the green economy outlook of Guangdong Province, China. Energy. https://doi.org/10.1016/j.energy.2020.118891.

[51] Cheng, Q., Liu, P., Xia, J., Ming, B., Cheng, L., Chen, J., Xie, K., & Li, X., 2022. Contribution of complementary operation in adapting to climate change impacts on a large-scale wind–solar–hydro system: A case study in the Yalong River Basin, China. Applied Energy. https://doi.org/10.1016/j.apenergy.2022.119809.

[52] National Energy Administration, 2024. Spanning east to west, stretching north to south, covering the entire nation, the national oil, gas, and electricity network is becoming increasingly dense. https://www.nea.gov.cn/2024-10/11/c_1310786436.htm [2025-08-30].

[53] Antonini, E. G. A., Ruggles, T. H., Farnham, D. J., & Caldeira, K., 2022. The quantity-quality transition in the value of expanding wind and solar power generation. *iScience*, *25*(4), 104140. https://doi.org/10.1016/j.isci.2022.104140.

[54] Zhang C.Y., Yang Y., Liu X., et al., 2023. Mobile energy storage technologies for boosting carbon neutrality, The Innovation, Volume 4, Issue 6, 2023, 100518, ISSN 2666-6758, https://doi.org/10.1016/j.xinn.2023.100518.

Highlights

- This study analyzed the net-zero power system with flexibility resources under climate change.
- A data-driven model for hourly load forecasting including key meteorological factors was built.
- China's electricity demand will reach 23262 TWh, and peak load will reach 3234 GW in 2060.
- Transmission and storage mitigate the spatiotemporal mismatch between renewable generation and load.

Declaration of interests

☒ The authors declare that they have no known competing financial interests or personal relationships that could have appeared to influence the work reported in this paper.

☐ The authors declare the following financial interests/personal relationships which may be considered as potential competing interests: